British Journal of Pharmacology

DOI:10.1111/j.1476-5381.2011.01268.x
www.brjpharmacol.org

RESEARCH PAPER

Protein kinase C–independent inhibition of arterial smooth muscle K^+ channels by a diacylglycerol analogue

RD Rainbow[1], AM Parker[2] and NW Davies[2]

[1]*Department of Cardiovascular Sciences, University of Leicester, Leicester, UK, and* [2]*Department of Cell Physiology and Pharmacology, University of Leicester, Leicester, UK*

Correspondence
NW Davies, Department of Cell Physiology and Pharmacology, University of Leicester, PO Box 138, Leicester LE1 9HN, UK.
E-mail: nwd@le.ac.uk

Keywords
potassium channels; dioctanoyl-sn-glycerol; vascular smooth muscle; protein kinase C; K_v channels; BK channels; K_{ATP} channels

Received
29 March 2010
Revised
1 November 2010
Accepted
17 January 2011

BACKGROUND AND PURPOSE

Analogues of the endogenous diacylglycerols have been used extensively as pharmacological activators of protein kinase C (PKC). Several reports show that some of these compounds have additional effects that are independent of PKC activation, including direct block of K^+ and Ca^{2+} channels. We investigated whether dioctanoyl-sn-glycerol (DiC8), a commonly used diacylglycerol analogue, blocks K^+ currents of rat mesenteric arterial smooth muscle in a PKC-independent manner.

EXPERIMENTAL APPROACH

Conventional whole-cell and inside-out patch clamp was used to measure the inhibition of K^+ currents of rat isolated mesenteric smooth muscle cells by DiC8 in the absence and presence of PKC inhibitor peptide.

KEY RESULTS

Mesenteric artery smooth muscle K_v currents inactivated very slowly with a time constant of about 2 s following pulses from –65 to +40 mV. Application of 1 μM DiC8 produced an approximate 40-fold increase in the apparent rate of inactivation. Pretreatment of the cells with PKC inhibitor peptide had a minimal effect on the action of DiC8, and substantial inactivation still occurred, indicating that this effect was mainly independent of PKC. We also found that DiC8 blocked BK and K_{ATP} currents, and again a significant proportion of these blocks occurred independently of PKC activation.

CONCLUSIONS AND IMPLICATIONS

These results show that DiC8 has a direct effect on arterial smooth muscle K^+ channels, and this precludes its use as a PKC activator when investigating PKC-mediated effects on vascular K^+ channels.

Abbreviations

Ang II, angiotensin II; BK channel, large conductance Ca^{2+}-activated K^+ channel; DiC8, 1,2 dioctanoyl-sn-glycerol; DMSO, dimethyl sulphoxide; K_v current, voltage-gated K^+ current; K_{ATP} current, ATP-dependent K^+ current; OAG, 1-oleoyl-2-acetyl-sn-glycerol; PKC-IP, protein kinase C inhibitor peptide 20–28

Introduction

Regulation of cytoplasmic calcium concentration ($[Ca^{2+}]_i$) is fundamental to the regulation of vascular tone (Jackson, 2000; Earley and Nelson, 2006). Elevations in $[Ca^{2+}]_i$, either by influx through voltage-gated Ca^{2+} channels or by release from intracellular stores, cause a contraction of arterial smooth muscle cells that ultimately results in an elevation of blood pressure (Nelson *et al.*, 1990; Jackson, 2000; McCarron *et al.*, 2006). The membrane potential and $[Ca^{2+}]_i$ in arterial smooth muscle are closely coupled with depolarization, leading to increased activity of voltage-gated Ca^{2+} channels and hence an increase in $[Ca^{2+}]_i$ and vascular tone. The relatively high permeability of the membrane to K^+, resulting from the

activity of several types of K^+ channels including large conductance calcium-activated potassium (BK) channels, ATP-sensitive potassium (K_{ATP}) channels, voltage-gated potassium (K_V) channels and inward rectifier potassium (K_{IR}) channels (nomenclature follows Alexander *et al.*, 2009), is the main factor setting the membrane potential (Standen and Quayle, 1998). Thus, activation of K^+ channels causes membrane hyperpolarization and vasodilation, while their inhibition contributes to depolarization (Nelson and Quayle, 1995; Jackson, 2000; Korovkina and England, 2002).

Many vasoconstrictors such as angiotensin II (Ang II) and endothelin-1 (ET-1) act via $G_{q/11}$-coupled receptors causing activation of phospholipase C (PLC), leading to production of inositol trisphosphate (IP_3) and diacylglycerol (DAG) from phosphatidylinositol bisphosphate (PIP_2) in the membrane. The resulting IP_3 causes Ca^{2+} release from sarcoplasmic reticulum Ca^{2+} stores, while DAG activates protein kinase C (PKC). Ang II and ET-1 have been shown to inhibit K_{ATP} and K_v channels in rat mesenteric arterial smooth muscle cells in a PKC-dependent manner (Clement-Chomienne *et al.*, 1996; Hayabuchi *et al.*, 2001a,b; Rainbow *et al.*, 2006; 2009). To investigate such mechanisms, analogues of DAG such as 1,2-dioctanoyl-sn-glycerol (DiC8) and 1-oleoyl-2-acetyl-sn-glycerol (OAG) have been used extensively as pharmacological activators of PKC. Several reports, however, show that some of these compounds can have additional effects that are independent of PKC activation. Bowlby and Levitan (1995) showed that DiC8 produces a direct block of $K_v1.3$ and $K_v1.6$ channels expressed in HEK293 cells, and L-type Ca^{2+} channels are also blocked directly by DiC8, though not by OAG (Kusaka and Sperelakis, 1995).

In this study, we describe experiments performed to investigate the action of the DAG analogue DiC8 on K_v, K_{ATP} and BK_{Ca} currents of rat arterial smooth muscle cells. We found that, in addition to actions consistent with activation of PKC, these compounds also had direct effects on K_v, BK and to a lesser extent K_{ATP} channels. Our results show that several K^+ channels are sensitive to PKC-independent block by DiC8 and demonstrate the need for caution when interpreting results obtained using DiC8 as a DAG analogue to activate PKC in smooth muscle preparations.

Methods

Preparation of vascular smooth muscle cells

All animal care and experimental procedures conformed to the requirements of the UK Animals (Scientific Procedures) Act 1986. Male adult Wistar rats (Charles River, Margate, Kent, UK) weighing 200–400 g were killed by cervical dislocation. Vascular smooth muscle cells from the mesenteric arteries were dissociated as follows. Arteries were removed and cleaned of blood and connective tissue in ice-cold solution containing (mM): 137 NaCl, 5.6 KCl, 0.42 Na_2HPO_4, 0.44 NaH_2PO_4, 1 $MgCl_2$, 2 $CaCl_2$, 10 HEPES and 10 glucose, adjusted with NaOH to pH 7.4. After dissection, the arteries were transferred to the same solution except that $CaCl_2$ was reduced to 0.1 mM (low-calcium solution) for 10 min and warmed to 35°C in a water bath. First, arteries were incubated for 31 min in low-calcium solution containing (mg·mL^{-1}): 0.9 albumin, 1.1 papain and 0.9 dithioerythritol. Then, the mesenteric artery was further digested for 12.5 min in low-calcium solution containing (mg·mL^{-1}): 0.9 albumin, 0.9 collagenase type F (Sigma, Poole, Dorset, UK) and 0.6 hyaluronidase type I-S (Sigma). Arteries were then transferred to low-calcium solution containing no albumin. Single smooth muscle cells were obtained by gentle trituration with a wide-bore pipette, stored at 4°C and used on the day of preparation.

Solutions and chemicals

For conventional whole-cell recordings, the intracelluar solution contained (mM): 110 KCl, 30 KOH, 10 HEPES, 10 EGTA, 1 $MgCl_2$, 1 $CaCl_2$, 1.0 Na_2ATP, 0.5 GTP; adjusted to pH 7.2. The free [Ca^{2+}], calculated using Maxchelator (http://www.stanford.edu/%7Ecpatton/maxc.html), was 20 nM. The 6 mM K^+ extracellular solution contained (mM): 134 NaCl, 6 KCl, 1 $MgCl_2$, 0.1 $CaCl_2$, 10 HEPES, 10 glucose; adjusted to pH 7.4. In some experiments, penitrem A (100 nM) was used to block BK_{Ca} channels. To record BK currents, the intracellular free [Ca^{2+}] was raised to 100 nm (3.84 mM $CaCl_2$). Single BK channels were recorded in excised inside-out patches exposed to intracellular solution containing 10 μM free Ca^{2+} using 10 mM N-(2-hydroxyethyl)-ethylenediamine-triacetic acid (HEDTA) as a chelator. The amount of total $CaCl_2$ added was calculated as above. The external solution was changed by continuous perfusion of the experimental chamber (volume 0.4 mL).

Data recording and analysis

Whole-cell and single channel currents were recorded from single smooth muscle cells using the patch clamp technique. Currents were recorded using an Axopatch 200A or 200B amplifier (Molecular Devices, Sunnyvale, CA, USA). Patch pipettes were made from thick-walled borosilicate glass (Clark Electromedical, Pangbourne, Berks, UK) using a pp-83 vertical puller (Narishige, Tokyo, Japan). Whole-cell currents were filtered at 5 kHz and single-channel currents at 2 kHz (–3 dB). Electrode resistances before sealing were 3–5 MΩ, and after sealing were >1 GΩ. Unless stated otherwise, all experiments were done at 30°C, maintained using a Dagan HW-30 temperature controller.

Tail currents, inactivation time constants and single channel data were analysed using custom software; otherwise, data were analysed using pClamp (Molecular Devices). Activation curves were fitted by a Boltzmann function:

$$activation = \frac{1}{(1+\exp((V-V_{1/2})/k))}$$

where $V_{1/2}$ is the membrane potential (V) at which half maximal activation occurs, and k is a factor determining the slope of the relation.

For single-channel analysis, a 50% threshold detection method was used, and a minimum resolution of 100 μs was imposed on the data before dwell times were binned according to the method of Sigworth and Sine (1987) at 25 bins per log unit. Bursts were identified as groups of openings separated by closings longer than a critical time. Gaps within bursts were assumed to arise from the two shortest time constants within the four or five components needed to fit the closed time distributions. The critical time was evaluated

such that the proportion of short gaps misclassified as long equalled the proportion of long gaps misclassified as short (see Colquhoun and Sakmann, 1985). Exponential distributions were fitted to the binned dwell times using the maximum likelihood method (Sigworth and Sine, 1987).

K_v current model

A model of K_v current block was developed based on the work of Zagotta *et al.* (1994). The calculations necessary to evaluate this model were done using in-house software developed to incorporate the matrix methods of solving such models described by Colquhoun and Hawkes (1982). The programme enabled current simulation using voltage protocols identical to those used during experiments, which was important when fitting model parameters to the data.

Data analysis

Data are expressed as means ± s.e.m. Intergroup differences were analysed by analysis of variance followed by Duncan's multiple range test or Student's *t*-test as appropriate. A value of $P < 0.05$ was considered statistically significant.

Materials

DiC8, OAG, penitrem A and pinacidil were purchased from Sigma. Myristoylated protein kinase C inhibitor peptide 20–28 (PKC-IP) was obtained from Calbiochem (Nottingham, UK). Glibenclamide was obtained from Tocris Biosciences (Bristol, UK). Some experiments were done using a membrane permeable Tat-linked PKC-IP supplied by Dr RI Norman.

DiC8 and OAG were dissolved in DMSO. The final concentration of DMSO was less than 0.2%.

Results

Whole-cell K_v, K_{ATP} and BK_{Ca} currents could be readily recorded from rat isolated mesenteric artery smooth muscle cells, albeit using different recording conditions optimized for each current. The conditions used for each current together with their properties and sensitivity to DiC8 are described below.

Properties of the voltage-dependent K^+ currents

Whole-cell patch clamp recordings from rat mesenteric artery smooth muscle cells revealed the presence of voltage-gated K^+ currents (K_v currents) induced by depolarizing steps to potentials more positive than about –30 mV (Figure 1). The current activated relatively slowly, and under control conditions, little inactivation was observed during 400 ms pulses. The relation between activation of the K_v current and membrane potential was obtained by analysing tail currents observed at –30 mV following a range of depolarizing steps from –65 mV. A single exponential function was fitted to these tail currents, and extrapolation of this function to the end of the test pulse was used as a measure of the instantaneous tail current amplitude. The activation data were obtained by normalizing tail current amplitudes to the maximum observed and plotted against test pulse potential (Figure 1C). These activation data were fitted with a Boltzmann distribution giving values for $V_{1/2}$ and k of –7.6 and 9.5 mV respectively.

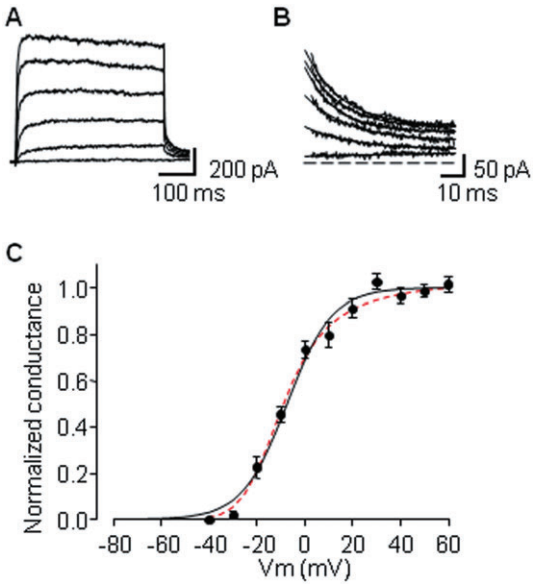

Figure 1

Activation properties of the K_v current in mesenteric artery smooth muscle. A. Family of currents observed following a range of pulses from –40 to +60 mV from a holding potential of –65 mV. At the end of each test pulse, the membrane potential was returned to –30 mV to obtain tail currents, which are shown expanded in part B; the solid line represents exponential fits to these tail currents. C. Plot of the normalized conductance obtained by normalizing the tail currents obtained at the various test potentials. Symbols show the mean ± s.e.m. from six cells. The solid line is the fit of the Boltzmann equation (Equation 1) to these data. The fit returned values of –7.7 and 9.4 mV for $V_{1/2}$ and *k* respectively. The dashed red line is the fit of the model to these data.

DiC8 produces a concentration-dependent inhibition of K_v currents

Application of DiC8 induced a marked increase in the rate of inactivation of K_v currents. In control conditions, K_v currents inactivated very slowly with a time constant (τ) of 1893 ± 121 ms at +40 mV (n = 6). This rate of inactivation was increased in a concentration-dependent manner by DiC8 (Figure 2A). Application of 1 μM DiC8 produced approximately a 40-fold increase in the rate of inactivation, decreasing τ to 44 ± 8 ms (n = 6) at +40 mV (Figure 2C). Since DiC8 is an analogue of DAG that has been used extensively to activate PKC, we examined whether the actions of DiC8 on the K_v current was due to its stimulatory effect on PKC. To test this, we preincubated smooth muscle cells with either 50 μM myristoylated PKC inhibitor peptide 20–28 (PKC-IP), or 50 nM Tat-linked PKC-IP, both of which are membrane permeable, for at least 15 min before measuring currents. We have shown previously that these treatments are effective at blocking PKC-dependent effects on these currents (Hayabuchi *et al.*, 2001b; Rainbow *et al.*, 2006; 2009). As shown in Figure 2B, the presence of PKC-IP had no effect on the ability of DiC8 to block K_v currents, and substantial inactivation was

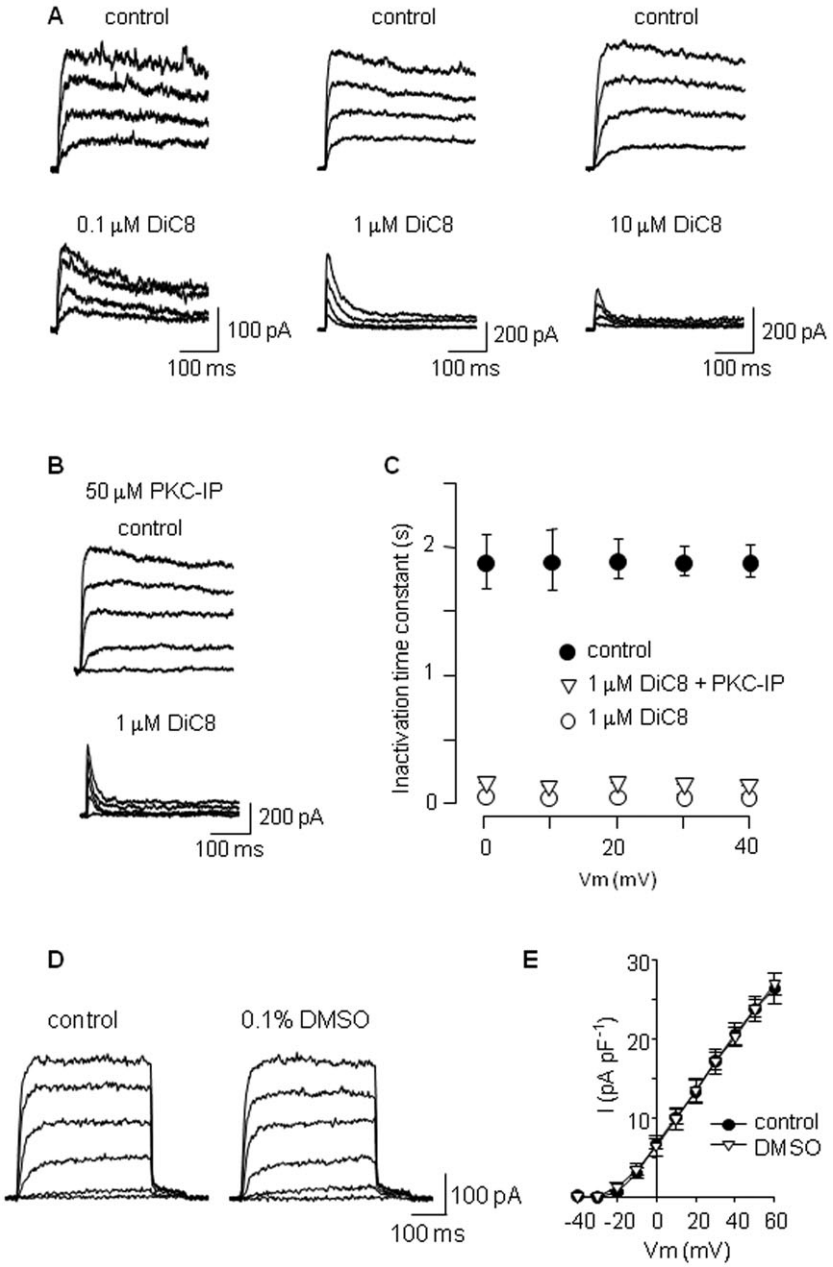

Figure 2

Direct effect of DiC8 on K_v currents. A. Typical K_v current traces under control conditions and in the presence of 0.1, 1 or 10 μM DiC8 as indicated. The currents shown were obtained during pulses from −65 to 0, +20, +40 and +60 mV. Note the increase in the rate of decay of the currents induced by DiC8. B. Preincubation of the cells for 15 min with 50 μM myristoylated PKC-IP in the pipette had little effect on the ability of DiC8 to inhibit the K_v current (pulses to −20, 0, +20, +40 and +60 mV). C. Plot of the time constants (mean ± s.e.m.) of K_v current decay over a range of pulse potentials under control conditions ($n = 6$) and in the presence of 1 μM DiC8 in the absence ($n = 6$) or presence of 50 mM PKC-IP in the pipette ($n = 6$). D. Typical K_v current traces under control conditions and in the presence of 0.1% DMSO as indicated. E. Mean current density against voltage from 3 cells in control and in the presence of 0.1% DMSO as indicated. DiC8, 1,2 dioctanoyl-sn-glycerol; PKC-IP, protein kinase C inhibitor peptide 20–28; DMSO, dimethyl sulphoxide.

still evident ($\tau = 153 \pm 13$ ms ($n = 6$) at +40 mV), indicating that this effect was mainly independent of PKC. Since DMSO was used to dissolve DiC8, we tested whether DMSO alone had an effect on K_v currents. The highest concentration of DiC8 used was 10 μM, which corresponded to a 0.1% solution of DMSO. In three out of three cells tested, we did not detect any effect on the K_v current of 0.1% DMSO (Figure 2D and E).

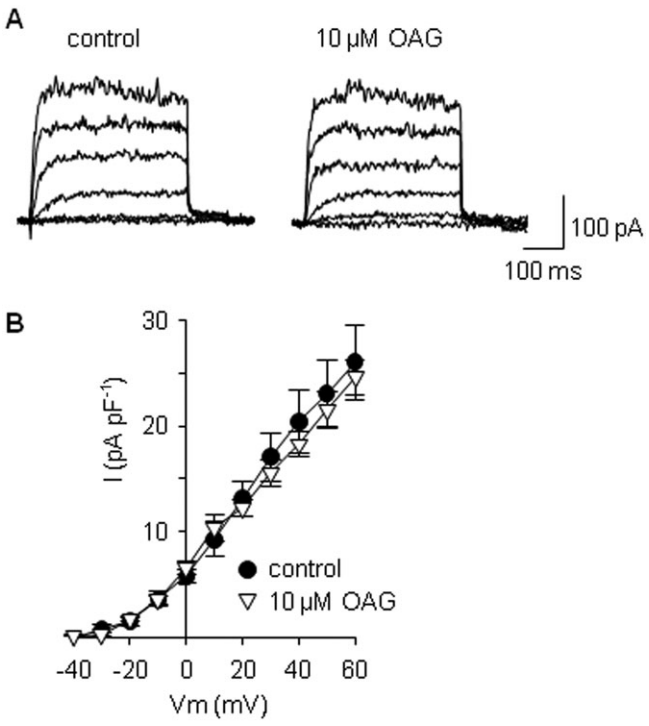

Figure 3

Lack of effect of OAG on K_v currents. A. Typical current traces under control conditions and following application of 10 μM OAG as indicated. B. Mean ± s.e.m. current density against voltage from four cells in control and in the presence of 10 μM OAG as indicated. OAG, 1-oleoyl-2-acetyl-sn-glycerol.

OAG does not mimic the effect of DiC8

OAG is an agent closely related to DiC8 that is also used as a DAG analogue and PKC activator. Application of 10 μM OAG had no effect on the K_v current (n = 4, see Figure 3). It is noteworthy that although OAG acts as a PKC activator, there was no detectable decrease in the K_v current, which is known to be inhibited by PKC activation in these cells.

The effect of DiC8 on K_v current is consistent with a state-dependent block

The rapid decline in K_v current following depolarizing pulses in the presence of DiC8 suggests a state-dependent block of the channels, as relief of block obviously occurred between pulses. To examine this in more detail, we measured the relative block, the rate of recovery from block and the rate of inactivation in the presence of DiC8 (see Figure 4). The relative block was expressed as fractional current obtained by measuring the mean currents over 50 ms at the end of the 400 ms pulses in the presence of 0.1, 1.0 or 10 μM DiC8 and normalizing these values to the current in control conditions. Initially, the block increased as membrane potential became more positive; however, above about +10 mV, there was no further increase in the amount of block, suggesting that the blocking rate itself is not voltage-dependent (Figure 4C). A plot of the apparent inactivation in the presence of DiC8 gives an indication of the rate of block. As seen in Figures 2B and 4E, the inactivation rates, particularly with 1 and 10 μM DiC8, did not vary greatly with voltage, again suggesting the actual blocking rate is not dependent on membrane potential. To measure the rate of relief from block at the holding potential of −65 mV in the presence of 1 μM DiC8, a 400 ms pulse to +40 mV was followed by a second pulse to the same potential after the membrane potential was returned to −65 mV for variable durations. A plot of the mean recovery of the blocked component against interpulse duration for five cells is shown in Figure 4D. The recovery followed an exponential time course with a time constant of 540 ms. These observations indicate that DiC8 blocks the K_v channel mainly, if not exclusively, in its open state. We explored this further by developing a model for the block of K_v currents by DiC8, though it should be noted that the K_v current in these cells does not arise from a homogeneous population of K_v subunits (Cox, 2005; see also Discussion).

Modelling the block of K_v currents by DiC8

To describe our data, a model has to simulate the activation characteristics of the control K_v current, including a slowly inactivating component; a block by DiC8 that is not in itself voltage-dependent but is clearly biased towards blocking the open state; and a relatively rapid relief of block upon returning to the holding potential. We based our model on the linear scheme shown in Figure 4A where the channel undergoes four transitions within closed states before opening, which is a simplified form of a more complete model proposed by Zagotta *et al*. (1994) and is termed a class B model by these authors. The transitions between the closed and open states are voltage-dependent and are given by:

$$\alpha = a(0).\exp(z_\alpha FV/RT)$$

$$\beta = \beta(0).\exp(-z_\beta FV/RT)$$

$$\gamma = \gamma(0).\exp(z_\gamma FV/RT)$$

$$\delta = \delta(0).\exp(-z_\delta FV/RT)$$

where α(0) is the rate at 0 mV, z_α is the equivalent charge movement accounting for the voltage dependence of the rate constant α, V is membrane potential and F, R and T have their usual thermodynamic meanings. It was necessary to reduce the transition from open to closed by a factor θ to account for K_v current deactivation (see also Zagotta *et al*., 1994). The other rate constants in the model (Figure 4A) were voltage-independent.

The model was fitted to the activation data presented in Figure 1 using a least squares minimization routine (see dashed line in Figure 1) while ensuring that current profiles were similar to those measured experimentally; final values for the rate constants and, where applicable, equivalent charge movements are presented in Table 1. To include the block by DiC8 in the model, we initially limited block to the open state only. While this could simulate much of our data, we found it necessary to allow C_4 and C_5, the two closed states just prior to the open state, and also the inactivated state to be blocked to give a better prediction of the effect of DiC8. For simplicity, we restricted the blocking and unblocking rates for each of these states to be equal. The reciprocal of the

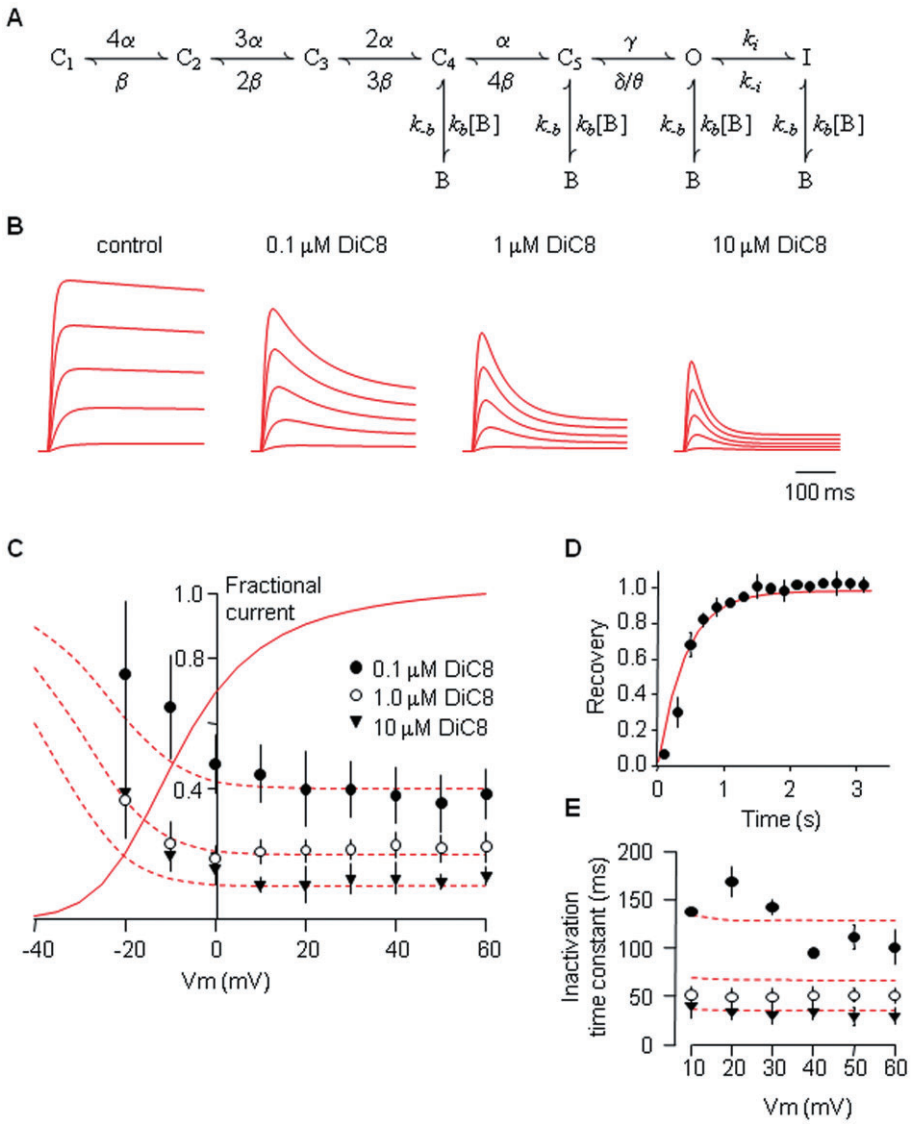

Figure 4

State dependence of the block of K_v currents by DiC8. In this figure, the red lines indicate the predictions given by the model. A. Kinetic scheme used to model DiC8 block of K_v currents. B. Current profiles given by this model for pulses to –20, 0, 20, 40 and 60 mV from a holding potential of –65 mV under the conditions indicated; values of the parameters used are given in Table 1 and in the text. C. Plot of the mean ± s.e.m. fractional current compared to control remaining at the end of 400 ms pulses in the presence of the DiC8 concentrations indicated. The dashed lines represent the fractional current predicted by the model, and the solid line is the activation curve given by the model (see also Figure 1). D. Plot of the recovery from block (mean ± s.e.m.) at the holding potential of –65 mV against time. E. Plot of the inactivation rate induced by DiC8 at the concentrations indicated. The symbols are as for part C, and the dashed lines are the predictions given by the model. DiC8, 1,2 dioctanoyl-sn-glycerol.

Table 1

Values of the parameters used in the model. The rate constants at zero potential [$V(0)$] are in ms^{-1}, while z represents the equivalent charge movement

	α	β	γ	δ	θ	k_i	K_{-i}
$V(0)$	0.151	0.050	0.116	0.246	12.4	2×10^{-4}	3.5×10^{-4}
z	0.261	1.145	0.061	0.542	–	–	–

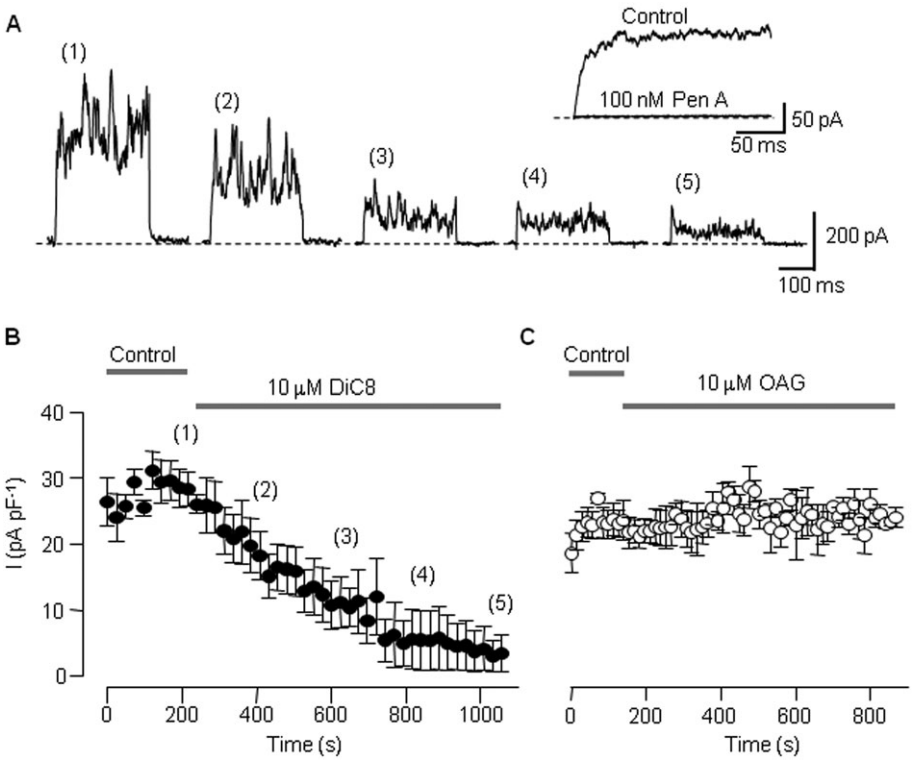

Figure 5

DiC8 but not OAG blocks BK currents in the presence of PKC-IP. A. Typical whole-cell current traces obtained following pulses to +80 mV from a holding potential of –20 mV. These records correspond to the times indicated in part B, with the first record obtained just before the addition of 10 µM DiC8. The spiky nature of the currents result from Ca^{2+} sparks activating BK channels in addition to the usual voltage-induced activation. The inset shows ensemble averages of 20 pulses from –20 to +60 under the same recording conditions in control and in the presence of 100 nM penitrem A as indicated. B. Time course of DiC8-induced inhibition of BK currents. Symbols show mean ± s.e.m. of six cells. The cells were preincubated with 50 nm Tat-PKC-IP for a minimum of 10 min before recording was commenced. C. Application of 10 µM OAG had no effect on BK currents (mean ± s.e.m., $n = 6$). DiC8, 1,2 dioctanoyl-sn-glycerol; OAG, 1-oleoyl-2-acetyl-sn-glycerol; PKC-IP, protein kinase C inhibitor peptide 20–28.

time constant for the recovery from block, 1.86×10^{-3}·ms^{-1}, was used as the starting value for $k_{-b,}$ the unblocking rate constant; to account for the recovery time course, the final value for k_{-b} was increased to 2.8×10^{-3}·ms^{-1} (see Figure 4E). It was necessary to set the overall blocking rate, k_b[B], for each concentration of DiC8 individually to obtain simulations that represented our data. The values used were 5×10^{-3}, 12×10^{-3} and 25×10^{-3}·ms^{-1} for 0.1, 1 and 10 µM DiC8 respectively (see Discussion). The red traces and plots in Figure 4 represent the calculations of the model with the values presented in Table 1 and in the text above. Our model was able to simulate the relative block of the current at the end of 400 ms pulses (Figure 4C), the rate of recovery from block at the holding potential (Figure 4D) and gave a reasonable prediction of the DiC8-induced inactivation (Figure 4E). Additionally, the current profiles shown in Figure 4B predict a decrease in the peak current in the presence of DiC8, a property that was evident in our experiments (see Figure 2).

DiC8 blocks BK channels

To investigate whether DiC8 was able to block other K^+ currents, we measured its effects on K_{ATP} and BK currents. Arterial smooth muscle cells express large numbers of BK channels, which can be observed during depolarizing pulses as a mixture of voltage-activated current and transient outward currents (STOCs). To investigate whether DiC8 affects BK currents in a PKC-independent manner, we preincubated cells for at least 10 min with 50 nM Tat-PKC-IP. Whole-cell recordings were obtained with 100 nM free Ca^{2+} in the pipettes. BK currents were activated following pulses to +60 mV from a holding potential of –20 mV (to minimize K_v currents). An example of the currents obtained from a cell before and during exposure to 10 µM DiC8 is shown in Figure 5A. It is evident that even in the presence of PKC inhibition BK current was reduced markedly by DiC8. The inset in Figure 5A shows that 100 nM penitrem A, a specific BK channel blocker, abolishes these currents, indicating that under these conditions, the currents induced result from the activation of BK channels. The plot shown in Figure 5B shows the time course and the extent of the inhibition measured in six cells. The currents, measured over the last 50 ms of the pulses, were normalized to cell capacitance. To test whether this effect was specific to DiC8, we repeated the experiment using OAG. As can be seen in Figure 5C, OAG had no effect on the BK current ($n = 4$). Furthermore, this result shows that

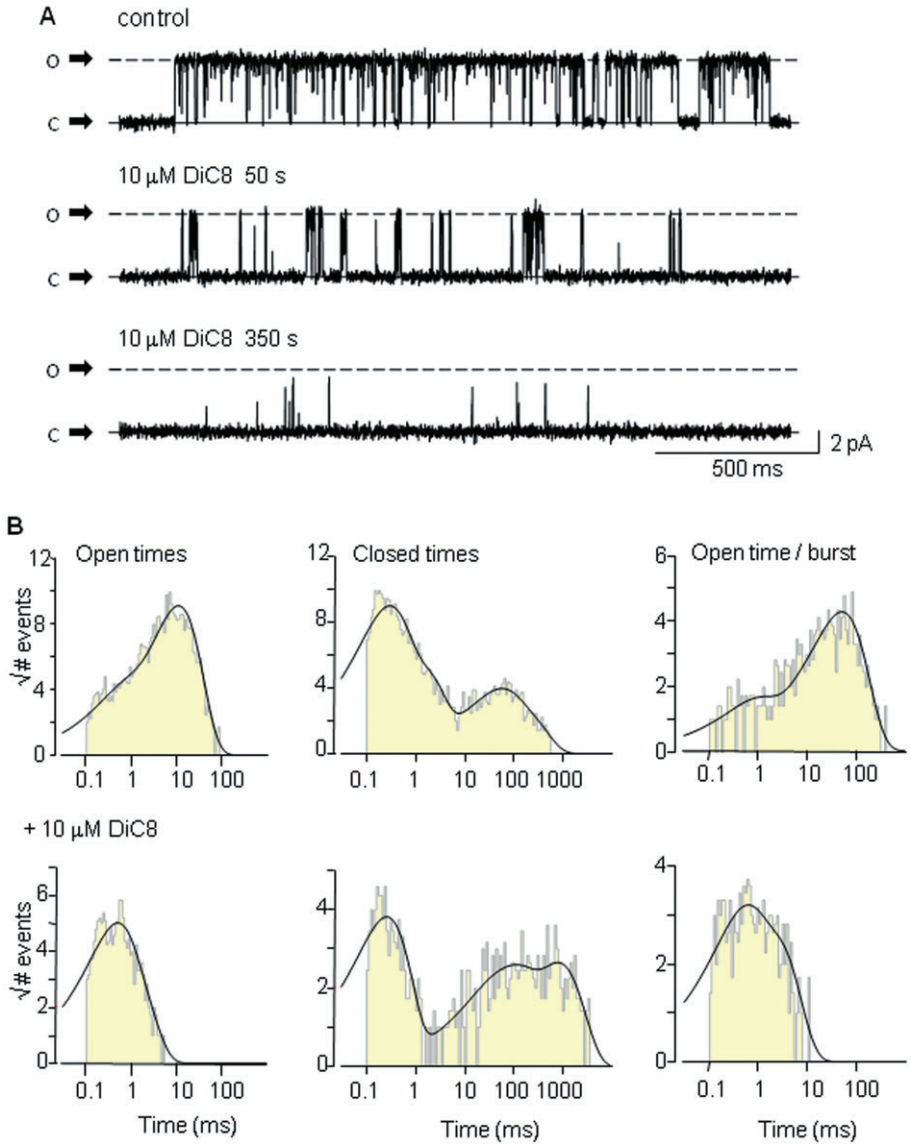

Figure 6

DiC8 applied to the cytoplasmic side of inside-out patches blocks the activity of BK channels. A. Sections of a recording made in an inside-out patch under control conditions (0 mV and a free [Ca^{2+}] of 10 μM) and after exposure of the patch to 10 μM DiC8 for 50 and 350 s. Open (O) and closed (C) levels are as indicated. B. Distributions of open times, closed times and total open time per burst in control conditions and in the presence of 10 μM DiC8. Mean open times, closed times and open times per burst were 7.9, 13.0 and 44.7 ms, respectively, in control and 0.5, 225.6 and 1.2 ms, respectively, in the presence of DiC8. The mean open times were corrected for missed closings as described in the methods. DiC8, 1,2 dioctanoyl-sn-glycerol.

the BK current does not run down with time and, since OAG was also dissolved in DMSO, that the inhibition of BK currents by DiC8 was not due to the presence of DMSO.

Block of single BK channels in excised inside-out patches

Because of the high expression of BK channels in smooth muscle cells, and the relative ease of recording these channels in excised patches, we investigated the effects of DiC8 on the activity of single BK channels. To ensure adequate activity of BK channels, inside-out patches were exposed to solutions containing 10 μM free Ca^{2+}. Mg^{2+} and ATP were excluded from these solutions to stop any phosphorylation events from occurring. Sections of recordings obtained from a patch containing a single BK channel are shown in Figure 6. Application of 10 μM DiC8 markedly reduced the activity, though as in the whole-cell experiments, the DiC8 had to be present for several minutes before substantial block occurred. Plots of the distribution of open times, closed times and total open time per burst for this patch, together with their fitted distributions, are shown in Figure 6B. DiC8 reduced mean open times and mean open times per burst but increased closed times, particularly the long closed durations. To establish

Table 2

Corrected mean ± s.e.m. open time and open time per burst in control (four patches) and in the presence of 10 μM DiC8 (five patches)

	Open time (ms)	Open time per burst (ms)
Control	5.91 ± 0.38	28.58 ± 5.68
10 μM DiC8	0.67 ± 0.06	2.21 ± 0.22

The values obtained are weighted according to the number of events in each patch (see Davies *et al.*, 1992).
DiC8, 1,2 dioctanoyl-sn-glycerol.

whether this was a classical open channel block, we compared the distributions of open time and total open time per burst in the absence and after at least 2 min exposure to 10 μM DiC8 (Table 1). As can be seen from Table 2, the total open time per burst in the presence of DiC8 is significantly shorter than the mean open time in the absence of DiC8 (*P*-value = 0.0011, un-paired *t*-test with Welch's correction for unequal variances). For a scheme involving a direct open channel block, where the channel must be unblocked before it can close, these two means ought to have the same value (Colquhoun and Hawkes, 1982). This, together with the delayed onset of action, indicates that the effect of DiC8 is unlikely to occur through a simple open channel block.

Effect of DiC8 on K_{ATP} channels

We also investigated whether DiC8 had a PKC-independent effect on K_{ATP} channels. Whole-cell K_{ATP} currents were recorded in symmetrical 140 mM $[K^+]$ at a holding potential of −60 mV. Application of 100 μM pinacidil, a K_{ATP} channel opener, ensured a robust activation of K_{ATP} current under these conditions. Figure 7A shows typical traces from two cells, one under control conditions and the other in a cell preincubated with myristoylated PKC-IP. Application of 1 μM DiC8 led to almost complete inhibition of the current as seen in the top trace. The arrows indicate when external $[K^+]$ was changed to 140 mM, and the resulting inward current is due to background activity of K_{ATP} channels. When cells were preincubated with PKC inhibitor peptide, DiC8 was still able to inhibit the pinacidil-induced K_{ATP} current, though not to the same extent as in the absence of PKC inhibitor peptide. Glibenclamide, a specific inhibitor of K_{ATP} channels, was added at the end of these experiments to verify that the current was due to K_{ATP} channels. In control cells, the pinacidil-induced K_{ATP} current was inhibited by 81 ± 3% by 1 μM DiC8, whereas those preincubated with PKC inhibitor peptide were inhibited by 51 ± 4% (Figure 7B, $P < 0.001$, unpaired *t*-test). These data suggest that there is a significant portion of the inhibition of K_{ATP} current in mesenteric smooth muscle cells by DiC8 that is PKC-independent.

We compared the inhibition of K_{ATP} current by DiC8 with that seen with OAG and Ang II. In the absence of PKC-IP, all three compounds reduced the K_{ATP} current by a similar amount. In the presence of PKC-IP, however, the inhibition by OAG and Ang II were reduced markedly, indicating that most of the inhibition by OAG and Ang II occurred through PKC activation. The level of inhibition of the K_{ATP} current by these three compounds was diminished in the presence of the PKC-IP ($P < 0.001$ for all, unpaired *t*-test).

Discussion and conclusions

In this paper, we show that DiC8, a diacylglycerol analogue used commonly to activate PKC, can block K_v, BK and K_{ATP} channels of mesenteric artery smooth muscle in a PKC-independent manner. Although a modest component of the block of K_{ATP} current was PKC-insensitive, we found that K_v and BK channels were particularly sensitive to PKC-independent block. Another DAG analogue, OAG, used commonly to activate PKC, had no effect on either K_v or BK currents, and, although it inhibited K_{ATP} currents, this inhibition was largely removed in the presence of PKC-IP. The lack of effect of OAG on K_v currents in the absence of PKC-IP may seem surprising, but we have shown recently that activation of mesenteric smooth muscle cells by either Ang II or ET-1 causes translocation of PKCα, PKCδ and PKCε (Nelson *et al.*, 2008), yet inhibition of K_v current by ET-1 and Ang II occurs only through PKCα and PKCε, respectively (Rainbow *et al.*, 2009), suggesting a much finer level of control than a general activation of PKC. DiC8 has been reported previously to block $K_v1.3$, $K_v1.6$ and *Shaker* mutant channels expressed in *Xenopus* oocytes and in HEK293 cells, independent of PKC activation (Bowlby and Levitan, 1995). In our experiments on K_v currents in rat mesenteric artery smooth muscle cells, the block by DiC8 was evident as a 40-fold increase in the apparent rate of inactivation (with 1 μM DiC8) that persisted when PKC was inhibited by PKC-IP. Mesenteric artery smooth muscle cells express several K_v channel subunits, including $K_v1.1$, K_v 1.2, K_v 1.5 K_v 1.6, K_v 2.1 and the K_v7 family in addition to the regulatory $K_v\beta1$ subunit (Cox, 2005; Mackie *et al.*, 2008; Moreno-Dominguez *et al.*, 2009). Under the conditions of our experiments, we did not detect K_v current at membrane potentials between −60 and −40 mV, a range where K^+ channels formed from K_v7 subunits are active (Mackie and Byron, 2008); nevertheless, it is very likely that the K_v currents recorded here comprise multiple K_v homo- or heterotetramers. Because the current recovered between pulses, we considered a mechanism whereby DiC8 interacted with the K_v channels in a state-dependent manner, and in particular, we were keen to ascertain whether a conventional open state block was sufficient to describe our data. To explore this, we developed a simple model whereby the K_v current was described by a single linear scheme comprised of five closed states and an open state where the rates connecting these states were voltage-dependent. In addition, to account for the slow inactivation seen under control conditions, an inactivated state was included. Although this model takes no account of the possibility that DiC8 may affect different K_v channel tetramers to varying degrees, it is noteworthy that $K_v1.3$, $K_v1.6$ and *Shaker* mutant channels were all blocked by DiC8 by an amount similar to that we report here for the K_v current of mesenteric artery smooth muscle cells (Bowlby and Levitan, 1995). Furthermore, the recovery from block (Figure 4D) followed a single exponential time course,

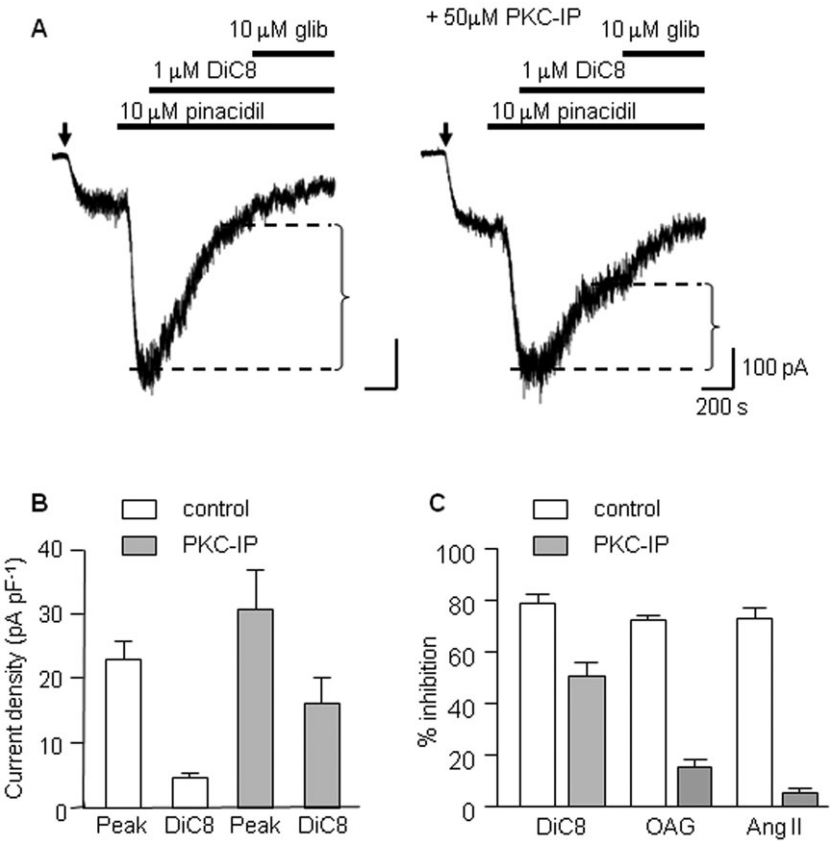

Figure 7

Block of K_{ATP} current by DiC8. K_{ATP} channels were recorded in symmetrical [K^+] at –60 mV and 10 μM pinacidil was used to activate them. The arrows indicate when external [K^+] was changed to 140 mM, and the resulting inward current is due to background activity of K_{ATP} channels. A. Application of 1 μM DiC8 led to almost complete inhibition of the current (left panel). Following preincubation with 50 mM PKC-IP, the inhibition by DiC8 was reduced (right panel). The measurement of DiC8 inhibition is indicated by the dashed lines. B. Mean pinacidil-induced current density before (peak) and after application of DiC8 in control cells and in cells preincubated with 50 μM PKC-IP as indicated. C. Mean inhibition (%, ±s.e.m.) of K_{ATP} current by 1 μM DiC8, 1 μM OAG and 100 nM Ang II in control conditions and in the presence of PKC-IP as indicated (n = 6 or 7 in each case). DiC8, 1,2 dioctanoyl-sn-glycerol. OAG, 1-oleoyl-2-acetyl-sn-glycerol; PKC-IP, protein kinase C inhibitor peptide 20–28.

suggesting that if different populations of K_v channels were blocked by DiC8, the unblocking rate was at least similar.

The best fit to the data was obtained by allowing the open state, the inactivated state and the two closed states C_4 and C_5 (Figure 4A) to be blocked. One interesting aspect of the model was that it was necessary to set the overall blocking rate for each concentration of DiC8 used. Having a constant value for the blocking rate constant and calculating the overall blocking rate as k_b.[DiC8] failed to fit the data. The values of the overall blocking rates used do not change in proportion to the change in concentration of DiC8 and indicate a discrepancy between the concentration applied in the bath and the effective concentration at the site of action. DiC8 is highly lipophilic; the virtual computational chemistry laboratory (http://www.vcclab.org) estimates DiC8 to have an average log*P*-value of 5.17, which suggests it is about 10^5 times more soluble in octanol than in water. It is therefore likely that DiC8 accumulates in the membrane at a much higher concentration than is present in the bathing solution, and it is possible that DiC8 approaches a saturating concentration within the lipid bilayer with relatively low aqueous concentrations.

Several reports indicate that lipid modification can alter ion channel activity (Smirnov and Aaronson, 1996; Crary *et al.*, 2000; Oliver *et al.*, 2004). Arachidonic acid causes a marked increase in the decay of delayed rectifier-type currents in pulmonary smooth muscle that was attributed to an effect that did not depend on PKC activation (Smirnov and Aaronson, 1996). In a study by Oliver *et al.* (2004), slowly inactivating $K_v3.1$ channels expressed in *Xenopus* oocytes can be induced to inactivate very quickly by the lipids arachidonic acid and anandamide. This alteration involved a change in the permeation of the channels and was attributed to modification of the pore structure with a possible contribution from changes in the mechanical properties of the lipid membrane (Oliver *et al.*, 2004). Studies using modification of DAG metabolism have shown that increasing endogenous DAG levels has a role in activating transient receptor potential (TRP) C3 channels (Venkatachalam *et al.*, 2003) and a cation current in rabbit ear artery (Albert *et al.*, 2005). It is not known whether DiC8 is mimicking any possible effect that increases in endogenous DAG levels may have on the channels investigated in this study.

Block of the BK channels by DiC8 in both inside-out patches and whole-cell currents accumulated over several minutes, suggesting a complex blocking mechanism. Furthermore, the total open time per burst in the presence of DiC8 was shorter than the mean open time in its absence, which is inconsistent with simple open channel block where both these parameters would be equal (Colquhoun and Hawkes, 1982). In a study of the block of cyclic nucleotide currents by DiC8, Crary *et al*. (2000) proposed two different mechanisms whereby DiC8 stabilized the closed state of this channel. In one mechanism, DiC8 interacted directly within hydrophobic crevices in the channel, and in the other, DiC8 was presumed to alter the mechanical properties of the lipid bilayer adjacent to the channel.

In summary, we have shown that the DAG analogue DiC8 was able to block K_v, BK and, to a lesser extent, K_{ATP} channels of rat mesenteric artery smooth muscle in a PKC-independent manner. This block is not seen with OAG, a related compound also used to activate PKC. Block of K_v channels appears to be state-dependent, with the block being relieved at negative potentials where the channels are closed. The results of single channel analysis of the block of BK currents suggest that it does not occur through a simple open channel block mechanism. In conclusion, care should be exercised when using DiC8 as a pharmacological tool to activate PKC, as phosphorylation-independent effects on several ion channels are likely to occur.

Acknowledgements

We thank Dr RI Norman for supplying the Tat-linked PKC inhibitor peptide and Mrs Diane Everitt for expert technical assistance. We also thank the British Heart Foundation for financial support.

Conflicts of interest

We declare no conflict of interest.

References

Albert AP, Piper AS, Large WA (2005). Role of phospholipase D and diacylglycerol in activating constitutive TRPC-like cation channels in rabbit ear artery myocytes. J Physiol 566 (Pt 3): 769–780.

Alexander SPH, Mathie A, Peters JA (2009). Guide to Receptors and Channels (GRAC), 4th edn. Br J Pharmacol 158 (Suppl. 1): S1–S254.

Bowlby MR, Levitan IB (1995). Block of cloned voltage-gated potassium channels by the second messenger diacylglycerol independent of protein kinase C. J Neurophysiol 73: 2221–2229.

Clement-Chomienne O, Walsh MP, Cole WC (1996). Angiotensin II activation of protein kinase C decreases delayed rectifier K^+ current in rabbit vascular myocytes. J Physiol 495 (Pt 3): 689–700.

Colquhoun D, Hawkes AG (1982). On the stochastic properties of bursts of single ion channel openings and of clusters of bursts. Philos Trans R Soc Lond B Biol Sci 300: 1–59.

Colquhoun D, Sakmann B (1985). Fast events in single-channel currents activated by acetylcholine and its analogues at the frog muscle end-plate. J Physiol 369: 501–557.

Cox RH (2005). Molecular determinants of voltage-gated potassium currents in vascular smooth muscle. Cell Biochem Biophys 42: 167–195.

Crary JI, Dean DM, Nguitragool W, Kurshan PT, Zimmerman AL (2000). Mechanism of inhibition of cyclic nucleotide-gated ion channels by diacylglycerol. J Gen Physiol 116: 755–768.

Davies NW, Standen NB, Stanfield PR (1992). The effect of intracellular pH on ATP-dependent potassium channels of frog skeletal muscle. J Physiol (Lond) 445: 549–568.

Earley S, Nelson MT (2006). Central role of Ca^{2+}-dependent regulation of vascular tone in vivo. J Appl Physiol 101: 10–11.

Hayabuchi Y, Davies NW, Standen NB (2001a). Angiotensin II inhibits rat arterial K_{ATP} channels by inhibiting steady-state protein kinase A activity and activating protein kinase Cε. J Physiol 530 (Pt 2): 193–205.

Hayabuchi Y, Standen NB, Davies NW (2001b). Angiotensin II inhibits and alters kinetics of voltage-gated K^+ channels of rat arterial smooth muscle. Am J Physiol Heart Circ Physiol 281: H2480–H2489.

Jackson WF (2000). Ion channels and vascular tone. Hypertension 35 (Pt 2): 173–178.

Korovkina VP, England SK (2002). Molecular diversity of vascular potassium channel isoforms. Clin Exp Pharmacol Physiol 29: 317–323.

Kusaka M, Sperelakis N (1995). Direct block of calcium channels by dioctanoylglycerol in pregnant rat myometrial cells. Mol Pharmacol 47: 842–847.

Mackie AR, Brueggemann LI, Henderson KK, Shiels AJ, Cribbs LL, Scrogin KE *et al*. (2008). Vascular KCNQ potassium channels as novel targets for the control of mesenteric artery constriction by vasopressin, based on studies in single cells, pressurized arteries, and in vivo measurements of mesenteric vascular resistance. J Pharmacol Exp Ther 325: 475–483.

Mackie AR, Byron KL (2008). Cardiovascular KCNQ (Kv7) potassium channels: physiological regulators and new targets for therapeutic intervention. Mol Pharmacol 74: 1171–1179.

McCarron JG, Chalmers S, Bradley KN, MacMillan D, Muir TC (2006). Ca^{2+} microdomains in smooth muscle. Cell Calcium 40: 461–493.

Moreno-Dominguez A, Cidad P, Miguel-Velado E, Lopez-Lopez JR, Perez-Garcia MT (2009). *De novo* expression of Kv6.3 contributes to changes in vascular smooth muscle cell excitability in a hypertensive mice strain. J Physiol 587 (Pt 3): 625–640.

Nelson MT, Quayle JM (1995). Physiological roles and properties of potassium channels in arterial smooth muscle. Am J Physiol 268 (Pt 1): C799–C822.

Nelson MT, Patlak JB, Worley JF, Standen NB (1990). Calcium channels, potassium channels, and voltage dependence of arterial smooth muscle tone. Am J Physiol 259 (Pt 1): C3–18.

Nelson CP, Willets JM, Davies NW, Challiss RA, Standen NB (2008). Visualizing the temporal effects of vasoconstrictors on PKC translocation and Ca^{2+} signaling in single resistance arterial smooth muscle cells. Am J Physiol Cell Physiol 295: C1590–C1601.

Oliver D, Lien CC, Soom M, Baukrowitz T, Jonas P, Fakler B (2004). Functional conversion between A-type and delayed rectifier K^+ channels by membrane lipids. Science 304: 265–270.

Rainbow RD, Hardy ME, Standen NB, Davies NW (2006). Glucose reduces endothelin inhibition of voltage-gated potassium channels in rat arterial smooth muscle cells. J Physiol 575 (Pt 3): 833–844.

Rainbow RD, Norman RI, Everitt DE, Brignell JL, Davies NW, Standen NB (2009). Endothelin-I and angiotensin II inhibit arterial voltage-gated K^+ channels through different protein kinase C isoenzymes. Cardiovasc Res 83: 493–500.

Sigworth FJ, Sine SM (1987). Data transformations for improved display and fitting of single-channel dwell time histograms. Biophys J 52: 1047–1054.

Smirnov SV, Aaronson PI (1996). Modulatory effects of arachidonic acid on the delayed rectifier K^+ current in rat pulmonary arterial myocytes. Structural aspects and involvement of protein kinase C. Circ Res 79: 20–31.

Standen NB, Quayle JM (1998). K^+ channel modulation in arterial smooth muscle. Acta Physiol Scand 164: 549–557.

Venkatachalam K, Zheng F, Gill DL (2003). Regulation of canonical transient receptor potential (TRPC) channel function by diacylglycerol and protein kinase C. J Biol Chem 278: 29031–29040.

Zagotta WN, Hoshi T, Aldrich RW (1994). Shaker potassium channel gating. III: Evaluation of kinetic models for activation. J Gen Physiol 103: 321–362.